Applied Radiation and Isotopes 127 (2017) 214–226

Contents lists available at ScienceDirect

Applied Radiation and Isotopes

journal homepage: www.elsevier.com/locate/apradiso

A preliminary study for the production of high specific activity radionuclides for nuclear medicine obtained with the isotope separation on line technique

F. Borgna[a,*], M. Ballan[b], S. Corradetti[b], E. Vettorato[a], A. Monetti[b], M. Rossignoli[b], M. Manzolaro[b], D. Scarpa[b], U. Mazzi[a], N. Realdon[a], A. Andrighetto[b]

[a] Department of Pharmaceutical and Pharmacological Sciences, University of Padua, Via Marzolo 5, 35131 Padova, Italy
[b] Laboratori Nazionali di Legnaro, Istituto Nazionale di Fisica Nucleare, Viale dell'Università 2, 35020 Legnaro, PD, Italy

HIGHLIGHTS

- The use of ISOL method for radionuclides production is proposed.
- ISOL method allows to produce carrier-free radionuclides for nuclear medicine.
- Tests with stable ion beams were produced as a proof of concept.
- Sodium Chloride is suitable as material for targets for Sr and Y beams.
- Activated Carbon can be compacted with PVA to have a solid target for I_2 beams.

ARTICLE INFO

Keywords:
Radionuclides
Radiopharmaceuticals
ISOL
SPES
Specific activity

ABSTRACT

Radiopharmaceuticals represent a fundamental tool for nuclear medicine procedures, both for diagnostic and therapeutic purposes. The present work aims to explore the Isotope Separation On-Line (ISOL) technique for the production of carrier-free radionuclides for nuclear medicine at SPES, a nuclear physics facility under construction at INFN-LNL. Stable ion beams of strontium, yttrium and iodine were produced using the SPES test bench (Front-End) to simulate the production of ^{89}Sr, ^{90}Y, ^{125}I and ^{131}I and collected with good efficiency on suitable targets.

1. Introduction

Radiopharmaceuticals are medicines that deliver a predefined amount of radiation to a target tissue for diagnostic or therapeutic procedures depending on the mechanism of decay. High penetrating radiation, such as γ emission, is mainly used for early diagnosis of tumors and inflammatory diseases (Azaiez et al., 2014). On the other hand particulate emission such as α and β^- emissions, which are capable of inducing cell death, are used for anticancer therapy and pathological conditions such as rheumatoid arthritis. The final goal of radionuclide therapy is to deliver a cytotoxic level of radiation onto a disease site (Handbook of Nuclear Chemistry, 2011).

Radiopharmaceuticals are consequently usually made of two parts: a "radioactive core" and a "carrier system"; the latter allows the deposition of radiation onto the malignant cell population thus avoiding damage to healthy tissues.

However, the physical production of the aforementioned "radioactive core" is regarded as one of the main problems. High costs of production, low reaction cross sections and product purity of current techniques are responsible for this difficulty. This is particularly true in the case of β^- emitting radionuclides.

These radionuclides are usually produced mainly by direct bombardment in dedicated targets using neutrons from nuclear reactors. By means of these reactions it is possible to produce a large number of isotopes and different nuclei in the target. The chemical methods to extract the desired radionuclide are not able to purify it from isotopic contaminants.

Thus specific activity, defined as the ratio between the activity (in terms of radioactivity) of the radioisotope and the mass of the element taken into account (Welch and Redvanly, 2003), is very low and carrier-added radionuclides are produced.

High specific activity is essential both for therapeutic and diagnostic radiopharmaceuticals. This fact should be especially emphasized in the case of radioimmunotherapy (RIT) and peptide receptor radionuclide therapy (PRRT), since cancerous cells have only a few selective sites. High specific activity is required to block these sites with tumor-seeking

* Corresponding author.
E-mail address: francesca.borgna@phd.unipd.it (F. Borgna).

http://dx.doi.org/10.1016/j.apradiso.2017.06.022
Received 2 November 2016; Received in revised form 22 April 2017; Accepted 14 June 2017
Available online 17 June 2017

Fig. 1. BestC70 cyclotron recently installed at LNL in the SPES building.

agents which carry the radioactive isotope and not the "cold isotope", which exerts no therapeutic effect (Welch and Redvanly, 2003).

The use of accelerators and beam purification techniques based on the ISOL (Isotope Separation On-Line) technique might be an efficient way to produce radionuclides for radiopharmaceutical applications; selecting different beams from a production target (mass selection) guarantees the possibility to produce carrier-free radionuclides.

2. ISOL method for the production of radiopharmaceuticals at SPES

The ISOL technique is already established as one of the main techniques for the on-line production of high intensity and high quality radioactive ion beams (Nilsson, 2013). The construction of SPES (Selective Production of Exotic Species) a second generation ISOL facility at INFN-LNL (Istituto Nazionale di Fisica Nucleare – Laboratori Nazionali di Legnaro) will allow the production of radioactive ion beams of neutron-rich nuclei with high purity in the mass range between 80 and 160 amu (Monetti et al., 2015).

At SPES the production of the radioactive isotopes is obtained by nuclear reactions induced by 40 MeV protons accelerated by a cyclotron, recently installed at LNL (Fig. 1), that collide with a multi-foil target consisting of disks of uranium carbide (UC_X) dispersed in carbon (Corradetti et al., 2013) and properly spaced in order to dissipate the deposited beam power (8 kW). The uranium contained in the target material will be ^{238}U, ensuring that the radioactive isotopes produced will belong to a group of elements having atomic numbers between 28 and 57 (elements placed between nickel and lanthanum in the periodic table). In particular, most of the produced nuclides will be neutron-rich, according to the chart of nuclides of Fig. 2.

The reaction products will be extracted from the target by evaporation at high temperature (about 2000 °C), and then forced through a transfer tube towards an ionization cavity where they will be ionized to the 1+ state (Manzolaro et al., 2013). Once ionized, these isotopes will be extracted and accelerated by means of at high potential (up to 40 kV). Radioisotope production and extraction from the target are represented in Fig. 3.

The resulting beam will be subsequently steered and focused using different electromagnetic systems and then finally purified in order to have a pure isotope beam without any contaminants. It will therefore be possible to collect the radionuclides of interest using a proper substrate placed at the end of the experimental line. A general scheme of the process is shown in Fig. 4.

The radioisotope production and collection performed with this technique have the capability to produce high specific activity materials using a simple procedure, meeting the requirements of radiopharmaceuticals. It is important to highlight that if the mass separation is performed effectively (ΔM/M at least better than 1/200) only an isobar chain is present in the collection target. The radiopharmaceutical quality is therefore expected to be extremely high. Using this production method, high specific activities, low gamma emitting impurities and very low isotope contamination can be expected. For this reason the ISOL technique is now under study for the production of radionuclides for nuclear medicine.

The radioisotopes produced at SPES using uranium carbide which are interesting from a radiopharmaceutical point of view are: ^{89}Sr (Kuroda, 2012), ^{90}Y (Goffredo et al., 2011), ^{125}I (Schwarz et al., 2012; Rodrigues et al., 2013; Shi et al., 2014), ^{131}I (Wyszomirska, 2012; Chamarthy et al., 2011) and ^{133}Xe (Mathews et al., 2008; Al-Busafi et al., 2012). Feasibility studies using stable ion beams for the production of strontium, yttrium and iodine are described later in this work.

3. ISOLPHARM

The ISOLPHARM project has the aim of performing, in the first instance, a feasibility study to use the RIBs produced at SPES as a new source of extremely pure radionuclides for use in nuclear medicine. The main aim is the obtainment of carrier-free radionuclides thanks to the mass separation followed by the chemical purification; the first process allows the removal of isotopic contaminants, the second of isobaric contaminants. To achieve this objective a wide range of knowledge must be taken into account, ranging from nuclear physics to engineering, technological production and radiopharmacy.

A profitable collaboration is now established between INFN-LNL and the Department of Pharmaceutical and Pharmacological Sciences of the University of Padua. The latter can provide the proper facilities for the chemical and pharmaceutical technological development of the project, so that from the very beginning a pharmaceutical production process can be developed.

It is important to clarify the main objectives of the project. The ISOLPHARM project initially is aimed at the production of radionuclides already present on the market, such as ^{89}Sr, ^{90}Y, ^{125}I, ^{131}I and ^{133}X. Nevertheless this can be regarded as innovative because of the possibility of producing them as carrier-free radionuclides. For example ^{89}Sr is produced by neutron irradiation and so it is carrier added, with very low specific activities values; it is for this reason used nowadays only in the chloride form (Metastron) as bone seeking agents for the palliation of bone metastases (Kuroda, 2012). Carrier-free ^{89}Sr produced with the ISOL method can be regarded as a new and innovative nuclide for molecule labeling and active targeting.

In the present work the results obtained from operating with stable beams already available at INFN-LNL are shown. The SPES test bench was used to produce stable strontium, yttrium and iodine beams, which simulate the production of ^{89}Sr, ^{90}Y, ^{125}I and ^{131}I.

As a second step, the ISOLPHARM project aims to study, as a research facility, the innovative radionuclides coming from a fissile target, as the one installed at SPES, bombarded with protons at high currents and energies. A broad fission spectrum can be obtained (see Fig. 2) and innovative radionuclides can be produced.

4. Experimental apparatus

The experimental apparatus present at LNL allowed the performance of some preliminary tests to verify the production of radionuclides of pharmaceutical grade with the ISOL technique. For this purpose, the SPES test bench, referred to as Front End offline (FE), was used. This apparatus, schematically represented in Fig. 5, has been designed and developed for the SPES project and is aimed at the production of (1+) ion beams. It is currently used in off-line mode, i.e. for the acceleration of stable ion beams; it is not connected to the proton beam line. Once the set up will be completed, it will be moved to a

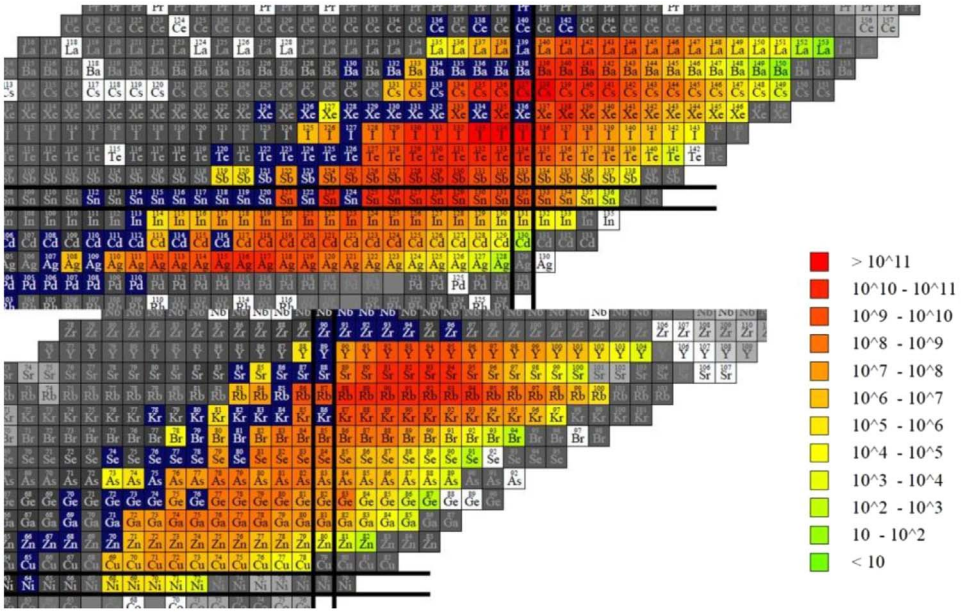

Fig. 2. Chart of the nuclides produced from ^{238}U fission target after irradiation with protons at the current of 200 μA and energy of 40 MeV. The numbers refer to the production in target. The blue squares represent the stable nuclides. (For interpretation of the references to color in this figure legend, the reader is referred to the web version of this article.)

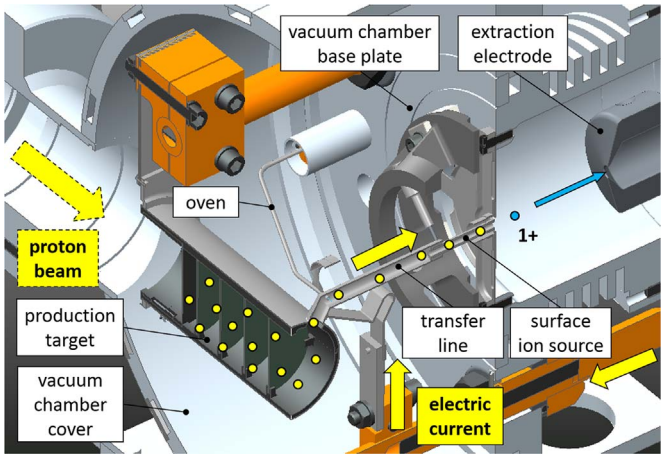

Fig. 3. SPES target layout. The proton beam coming from the left of the picture is impinging on the multifoil $^{238}UC_x$ target. Produced isotopes can exit the target through the transfer line and be ionized (in this picture a Surface Ion Source is outlined) and extracted. All of the target system is heated (2000 °C) and under high vacuum conditions.

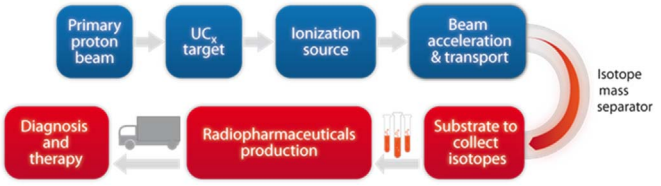

Fig. 4. The process for the production of radionuclides and their use for radiopharmaceutical production is described. The blue balloons concern the nuclear physics steps, from the mass separation on (red balloons) the pharmaceutical aspects for the production have to taken into account. (For interpretation of the references to color in this figure legend, the reader is referred to the web version of this article.)

Fig. 5. Schematic representation of the Front End off-line with its main components. FC1 and FC2 are the two Faraday Cups, diagnostic devices, placed before and after the Mass Separation system (the Wien Filter).

dedicated bunker in the final SPES building and coupled to the cyclotron line.

To study the production of a radionuclide with the ISOL technique to obtain radiopharmaceutical products, stable isotopes of the same element can be a good alternative, since they have the same chemical behavior. For this reason the FE was used to produce stable ion beams to carry out the feasibility tests reported here.

The FE has been extensively described in previous papers (Manzolaro et al., 2014). Briefly, it is made of five main functional subsystems: the ion source complex, the beam optics subsystem, the Wien filter, the diagnostic boxes 1 and 2. The ion source complex is placed inside a vacuum chamber that enables the use of the ion source at high temperatures with pressure levels between 10^{-5} and 10^{-6} mbar. In offline mode, no fissile target is installed inside the chamber but different methodologies are used to introduce the stable isotopes to be ionized and accelerated depending on the physical state of the element. In the case of gases, they are introduced through a controlled gas flow and injected in the ionization source by means of a calibrated leak; in case of solid materials, they are usually soluble salts, dissolved in acidic media and quantitatively deposed and solvent evaporated on a tantalum foil, called the mass marker (MM). The mass marker is then carefully folded (Manzolaro et al., 2013) and inserted into a heated tantalum tube, called the oven, that allows the element atomization and injection into the ionization source. The ionization sources used in the experiments later described are of two kinds, depending on the first ionization potential of the element (Manzolaro et al., 2014, 2016). For elements of the 1st and 2nd group, the Surface Ion Source (SIS) is adopted; for those with higher electronegativity, the Plasma Ion Source (PIS) is required.

The SPES SIS, see Fig. 6, is a hot-cavity ion source and its components are mainly made of tantalum (Manzolaro et al., 2013). Geometric specifications of the SIS ion source used to perform tests are reported by Manzolaro et al. (2016). Surface ionization occurs following the interaction of the atoms with a heated surface; the interaction causes the loss of an electron and the production of a positive singly charged ion. This mechanism (Wolf, 1995) is good only for elements with a first ionization potential smaller than 7 eV and with a hot-cavity made of materials with high work function values (like tantalum) (Al-Khalili and Roeckl, 2006). The operating temperature of the source is a crucial parameter to achieve an effective ionization.

The second kind of ion source used in the tests is the SPES PIS, which is a forced electron beam induced arc discharge ion source

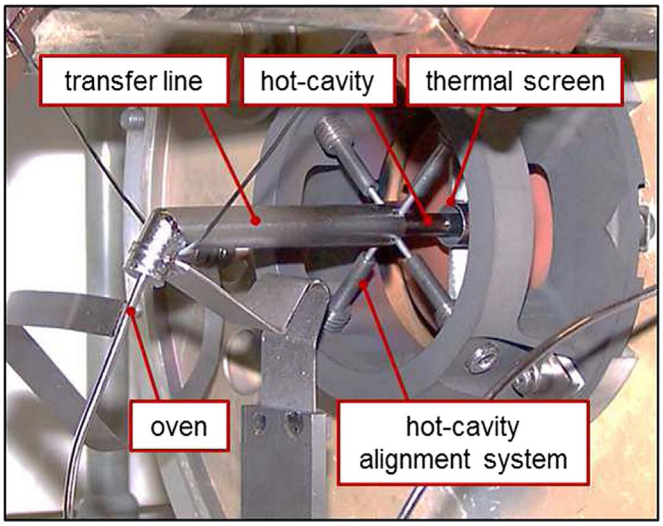

Fig. 6. A picture of the SPES Surface Ion Source (SIS). This layout is used for the off line tests, the transfer line is connected to the oven, the tantalum tube used to introduce stable atoms into the source for ionization. The component indicated as hot cavity is the hottest region of the source, the one responsible for atoms' ionization. With SIS only low ionization potential elements can be ionized, in particular those belonging to 1st and 2nd group.

(Manzolaro et al., 2016, 2014). It is a non-selective device capable of ionizing a large spectrum of elements, mainly composed of two parts: the tantalum cathode and the molybdenum anode. The former is heated at 2200 °C by the Joule effect, generating an intense thermionic emission of electrons (free electrons) on the cathode surface facing the anode. The anode, at 150 V with respect to the rest of the ion source, attracts the ionizing electrons, in this way allowing the creation of a plasma inside its cylindrical cavity. PIS is also suitable for ionization of elements with high first ionization potential.

The ion source is placed on a 25 kV platform with respect to the extraction electrode at ground potential. The high voltage can however be increased to 40 kV. The beam optics subsystem is made of a set of electrostatic deflectors and a quadrupole triplet that allow for beam alignment and focusing, respectively. In diagnostic box 1 there is a Faraday cup for beam intensity monitoring and a grid-based beam profile detector.

The beam mass selection is performed by a Wien Filter (Wien, 1897, 1902) a device which is able to select a specific ion due to mutually perpendicular electric and magnetic fields orthogonal to the ion velocity. The undeflected particles have speed equal to the ratio between electric and magnetic field. The deflected ions are then stopped by a slits subsystem. Since the various masses have approximately the same energy (25 keV), this device can be used in the SPES Front-End as a mass selector. For this reason, the Wien Filter is composed by a vacuum chamber where two electrodes, maintained at a certain potential, provide the desired electric field and by a magnet excited by two coils, that supplies the magnetic field.

Following mass separation, a second diagnostic box is installed, constituted by a Faraday cup, a grid-based beam profile detector and an emittance meter device.

For the simulation of the radionuclide production for the development of radiopharmaceuticals, a substrate of pharmaceutical grade is positioned at the end of the line, immediately after the emittance meter in order to collect the desired accelerated stable ions.

5. Experimental activities description

5.1. Materials

Strontium Standard for AAS *TraceCERT* (Fluka Analytical) was used for the production of strontium ion beams and for strontium analysis via AAS for standards preparation. Sodium Chloride *TraceSELECT* (Fluka Analytical) was used for strontium beam deposition. Yttrium Standard for AAS *TraceCERT* (Fluka Analytical) and Yttrium Chloride hexahydrate 99,99% trace metal basis (Sigma Aldrich) were used for ytrrium beam production and Sodium Chloride (Sigma Aldrich) was used for yttrium deposition. Nitric Acid 69,0% TraceSELECT (Fluka Analytical) was used for sample preparation in strontium and yttrium analysis. Active charcoal Carbo Activatus USP (A.C.E.F.) and Poly(vinyl alcohol) AMw 31,000–50,000, 98–99% hydrolyzed (Sigma Aldrich) were used for the production of the substrate to collect iodine beams.

Formic acid 99–100% AnalaR Normapur Analytical reagent (Prolabo), Sulfuric Acid 95–97% for analysis or manufacturing use (J.T. Baker), Bromine reagent grade (Sigma Aldrich), Potassium iodate 99.5% for analysis (ACROS Organics), Potassium iodide puriss p.a. reag. ISO, reag. Ph. Eur. 99.5% (Sigma Aldrich)

and Sodium thiosulphate solution 0.1 mol/L (Scharlab S.L.) were used for iodine analysis. Sodium hydroxide reagent grade 98%, pellets (anhydrous) (Sigma-Aldrich) was used for iodine extraction from the substrate prior to analysis.

5.2. Mass marker technique

The Mass Marker capillary technique (Schwellnus et al., 2009) is a useful method for the introduction of atoms into the front end. It is used to simulate the process of diffusion of radioactive isotopes towards the ionization source in the off line tests. It consists of a small tantalum foil (mass marker) on which a calibrated volume of the solution containing the element is placed. The solution is allowed to evaporate, leaving on the marker only the salt (Crepieux and Kirkby, 2006); then it is accurately folded and introduced inside a tantalum tube, called the oven. The diffusion process is regulated by the temperature and by the vapour pressure of the introduced molecule, that is why the oven is heated by means of Joule effect, a well established method to heat components of that kind (Manzolaro et al., 2010) and the temperature can be regulated so as to control the diffusion process (Manzolaro et al., 2013).

For strontium beam production a volume ranging from 40 to 140 μL of a standard solution of strontium nitrate (1 g/L) was added on the Mass Marker and introduced into the Front End. For iodine beams a solution of potassium iodide (1 g/L) was used: volumes used ranged from 40 to 150 μL. In the case of yttrium, two different chemical salts of the element were used: yttrium nitrate and yttrium chloride. In both cases 900 μL of the solutions were placed on the tantalum foil that was not folded, but directly introduced in the transfer line of the ionization source to facilitate evaporation.

5.3. Substrates production

Sodium chloride disks were produced for strontium and yttrium beam collection. The disks were obtained by pressing different amounts of sieved (300 μm) NaCl powder in an industrial press. The mold die had a diameter of 40 mm and a force of 30 t was applied for 5 min; no ligand was used. For the deposition of strontium, the disks were produced by pressing sodium chloride TraceSELECT to avoid traces of strontium present as contaminants in the others. For yttrium deposition, pure sodium chloride was not needed, since no yttrium traces are present.

Different quantities of powder from 1.8 g to 3.6 g were compressed and tested for mechanical resistance, using a texture analyzer (TA-HDi - Stable Micro System). The measurement was carried out by setting the lowering of the probe to 40% of the disk thickness. Prior to the deposition experiments, the disk was fixed on a tailored support on a flange at the end of the FE, as shown in Fig. 7.

For iodine deposition activated carbon was chosen as the secondary target material. Sodium chloride contains iodine as an intrinsic contaminant, so it could not be used. Moreover, iodine is in the gaseous

Fig. 7. The final deposition substrate used for strontium and yttrium beams deposition. The sodium chloride compact matrix is fixed with a Teflon disk on a flange that can be easily assembled and placed in the last part of the FE.

state at the working pressure (10^{-5} – 10^{-6} mbar) (Honig, 1962), so a material able to trap it was chosen (Haefner and Tranter, 2007; Wilhelm and Deuber, 1991; Paviet-Hartmann et al., 2010). To obtain a solid and compact matrix, different ligands were considered: cellulose derivatives, lipophilic ligands, sugars and polymers. For the first two categories direct compression of the powders was performed, using different amounts of ligand (15% and 30% of microcrystalline cellulose, 3% of stearic acid) (Rowe et al., 2012). In the case of sugars, in particular sorbitol, a pre granulation process was adopted. Activated carbon was pre granulated with a 10% and 30% p/v sorbitol solution and heated to dryness (40 °C all night). The granules thus produced were then compacted.

In the case of polymers, instead, a convenient hot pressure process had to be established. Poly Vinyl Alcohol (PVA) promises to be a good ligand for activated carbon (Lozano-Castelló et al., 2002). In this case different percentages of PVA were tested, following a pre granulation process. Powder compression was carried out, after having manually ground and sieved the granules, for 10 min at 180 °C and applying 2 t on a mold of 40 mm of diameter. The overall procedure for the production of AC/PVA disks can be summarized as follows:

1. Activated carbon wetting with an aqueous solution of PVA (5% w/v) until obtainment of a wet mass;
2. Drying overnight in a stove at 60 °C;
3. Repetition of task 1 until the desired percentage of PVA (50%) was obtained;
4. Drying overnight in a stove at 60 °C;
5. Sieving and grinding of the obtained granules (sieve 300 μm);
6. Compacting of about 1 g of powder in a pre-heated mold at 180 °C for 10 min, 2t;
7. Conservation of the obtained disks in argon atmosphere to avoid exposure to humidity.

The obtained activated carbon-PVA (50% m/m) disks were characterized for morphology, specific surface area, mechanical resistance and weight loss in a vacuum.

- To characterize the disk surface morphology, SEM (Scanning Electron Microscopy) was performed using a Tescan Vega 3xmh;
- To verify porosity and specific surface area, a physisorption analyzer was used (Micromeritics ASAP 2020);
- Mechanical resistance and weight loss in vacuum were tested as for sodium chloride matrixes.

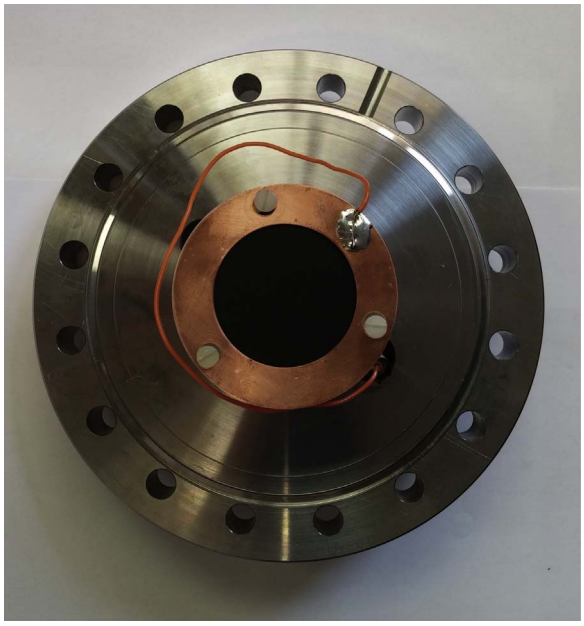

Fig. 8. AC/PVA disk on the final support form iodine beams deposition. The copper ring sustains the disk and allows the measurement of the iodine current impinging on the collecting substrate.

PVA could present some chemical incompatibilities with iodine due to the possible formation of a complex (Moulay, 2013). To verify it, a small amount of iodine was added to a solution of PVA at basic pH obtained by adding NaOH, and analyzed with a UV spectrophotometer (Varian, Cary 50 Scan), λ_{max} = 490 nm, to verify if the complex was formed at those conditions.

Also in this case the substrate was fixed on a support at the end of the beam line for the collection of the accelerated ions, as shown in Fig. 8. In this case the support was used as a third Faraday Cup, as later explained.

5.4. Strontium, yttrium and iodine quantification

An analytical method has been established for each element in order to quantify the effective number of atoms deposited on the substrate after beam irradiation; both the nature of the element and of the matrix has been taken into consideration.

In the case of sodium chloride disks, after irradiation they were dissolved in a proper solvent for chemical quantitative analysis.

For strontium the disk was dissolved in 400 mL of HNO_3 0.3 M and analyzed via Atomic Absorption Spectroscopy with atomization in a Graphite Furnace (GF-AAS), (GTA 110 with PSD 120 auto sampler, Varian) and a hollow cathode lamp for strontium (Heraeus) with operating wavelength 460 nm. In order to obtain an accurate and reproducible method, a strong acidic matrix was used (HNO_3 0.3 M); after disk dissolution sodium chloride coming from the disk was a great interfering agent, because of non specific absorbance phenomena. A large excess of nitric acid leads to the formation of $NaNO_3$, high volatility products, that evaporate under 500 °C (Frech and Cedergreen, 1977). The calibration curve method was used for sample quantification. Four standards were prepared (5, 10, 15 and 20 μg/L) and analyzed prior to sample analysis. The calibration curve in Fig. 12 was obtained (r^2 = 0995) and used for strontium quantification.

For yttrium a different analytical method was chosen since, due to its low volatility, it can not be observed with AAS (Prell and Styris, 1991). ICP-OES (Inductive Coupled Plasma-Optic Emission Spectroscopy) was chosen. In order to minimize the quantity of sodium, disks of 1.8 g of NaCl were used for beam deposition.

The analytical method was found to be linear in the concentration

range, sensitive, accurate and precise. Standards were prepared at 2 μg/L, 7 μg/L, 10 μg/L and 70 μg/L using HNO_3 0.1 M + NaCl 18% to obtain the same matrix of the sample. The irradiated sodium chloride disk was dissolved in 10 mL of HNO_3 0.1 M, because this was the smallest volume capable of entirely dissolving the disk. For each concentration 3 measures were taken and data fitted to obtain calibration curve. Yttrium characteristic λ are: 371.030 nm, 360.073 nm and 377.433 nm. In order to choose the best analyzing wavelength, precision, accuracy and the limit of detection (LD) were taken into account (Di Noto et al., 1995). 371.030 nm was chosen as the best wavelength for yttrium quantification.

For yttrium analysis it was possible to dissolve the disk in a much smaller volume because the ICP analysis was much less affected by the presence of NaCl. So the analysis could be carried out with minor dilution of the sample.

In the case of iodine quantification, a process was developed to extract iodine deposited in the carbon matrix. As reported in literature (Kaghazchi et al., 2009) basic solutions from NaOH can efficiently extract iodine from activated carbon, after I_2 dismutation in basic solutions. 10 mL of a 0.5 M solution of NaOH were mixed with the irradiated substrate in order to dissolve iodine. For the first 2 deposition tests the process was carried out at room temperature for 15 min. For the 3rd one the temperature was increased to 55 °C and the contact time between NaOH and the substrate was 120 min. The solution was then treated with 1 M sulfuric acid in order to obtain an acidic pH (pH~5). The solution was then automatically titrated (848 Titrino Plus – Metrohm) with sodium thiosulfate 0.001 M, after pretreatments with bromine water, formic acid and an excess of potassium iodide. Titration proved to be accurate and sensitive enough for iodine quantification.

5.5. Ion beams deposition

Using the aforementioned apparatus and techniques, strontium, yttrium and iodine beams were produced and collected on the described substrates, shown in Figs. 7 and 8. In Table 1 the main experimental conditions are listed for each element.

Before carrying out the depositions, ionization efficiency and focalization tests were performed.

Ionization efficiency tests were carried out by evaporating the material contained in the mass marker (40 μL) and, after ionization and acceleration, collecting the beam in the second Faraday Cup. By integrating the curve of current over time the number of ionized atoms can be obtained; this quantity can be divided by the number of atoms introduced in the MM to obtain ionization efficiency. To check qualitatively the accelerated beam, several mass scans using the Wien Filter were performed.

The emittance meter was used to control beam dimensions, position and divergence for each element and to set the deflectors and quadrupoles voltage in order to maximize the beam impinging the target disk.

In the cases of strontium and yttrium, the beam current could not be continuously monitored during the deposition experiments, because all diagnostic instruments were remotely removed from the beam line, since they would have stopped the beam. The beam current was however periodically checked by introducing the secondary Faraday Cup for a few seconds. In the case of iodine, the substrate itself, being composed of a conductive material, was used as a third Faraday Cup, allowing the monitoring of iodine current throughout the deposition.

6. Results

6.1. Substrate production and characterization

Sodium chloride, as a material for beam deposition, promises to be ideal because it is completely biocompatible with human administration. It can be taken orally or injected. It has also good solubility properties, allowing its possible dissolution in biocompatible media after beam trapping.

Following the compression of sodium chloride powder, disks of 40 mm of diameter were obtained. Mechanical resistance proved to be sufficient for disks heavier than 1.8 g (strength at break > 64.00 ± 0.16 N). No weight loss was observed after placing the disks in high vacuum for several days, suggesting that the humidity uptake was negligible.

Hot compression of activated carbon with 50% (w/w) of PVA proved to be the only method to obtain solid and resistant substrates for iodine beam deposition.

As for sodium chloride, the activated carbon/PVA disks were tested for mechanical resistance. Three disks were tested: the first disk presented poor mechanical resistance strength at break 9.19 N, while the second two samples were broken after applying a strength higher than 92 N. This probably comes from the fact that the first one was not conserved in argon atmosphere and it absorbed water from the atmosphere. Indeed, when this disk was placed in high vacuum for several days it had a weight loss of 2.4%. The disk stored in argon atmosphere instead had a weight loss of 0.9%.

SEM analysis allowed verifying the disks homogeneity, both on the surface and in the interior, as shown in Fig. 9a and b.

Compression did not affect material porosity: the specific surface area of the disk was 190 m^2/g, equivalent to that of the powder before compression.

6.2. Ion beam production and deposition with the Front End

The number of atoms impinging the secondary target is solely dependent on two main variables: the ionization efficiency (ε_i) and the selection efficiency (ε_s). Thus, the number of atoms can be calculated as follows:

$$N_t = N_{MM} \bullet \varepsilon_i \bullet \varepsilon_s, \quad (1)$$

where N_t is the total number of ions reaching the target, N_{MM} is the number of atoms introduced in the MM, and ε_i and ε_s are the ionization and separation efficiency respectively.

6.2.1. Strontium

When 40 μL of strontium standard solution were loaded in the mass marker, an ionization efficiency of about 10% ($\varepsilon_i = 0.1004$) was obtained. The number of atoms introduced in the Mass Marker (N_{MM}) was $2.75 \cdot 10^{17}$ and the number of ions detected in the FC1 (N_i) were

Table 1
Main experimental conditions for the ionization and deposition experiments carried out for the three elements under study.

	Strontium	Yttrium	Iodine
Ionization source	Surface Ion Source	Plasma Ion Source	Plasma Ion Source
Starting chemical form	Strontium nitrate	Yttrium chloride	Potassium iodide
Mass marker placement	Oven	Transfer line	Oven
Solution loaded in the mass marker	Strontium nitrate solution (1 g/L), 140 μL	Yttrium chloride (1 g/L), 900 μL	Potassium iodide (1 g/L), 150 μL
Secondary target	Sodium chloride 3.6 g	Sodium chloride 1.8 g	Activated carbon 50% (w/w) PVA 50% (w/w) 1.3 g
Analytical technique	GF-AAS (λ = 460.70 nm)	ICP-OES (λ = 371.03 nm)	Titration

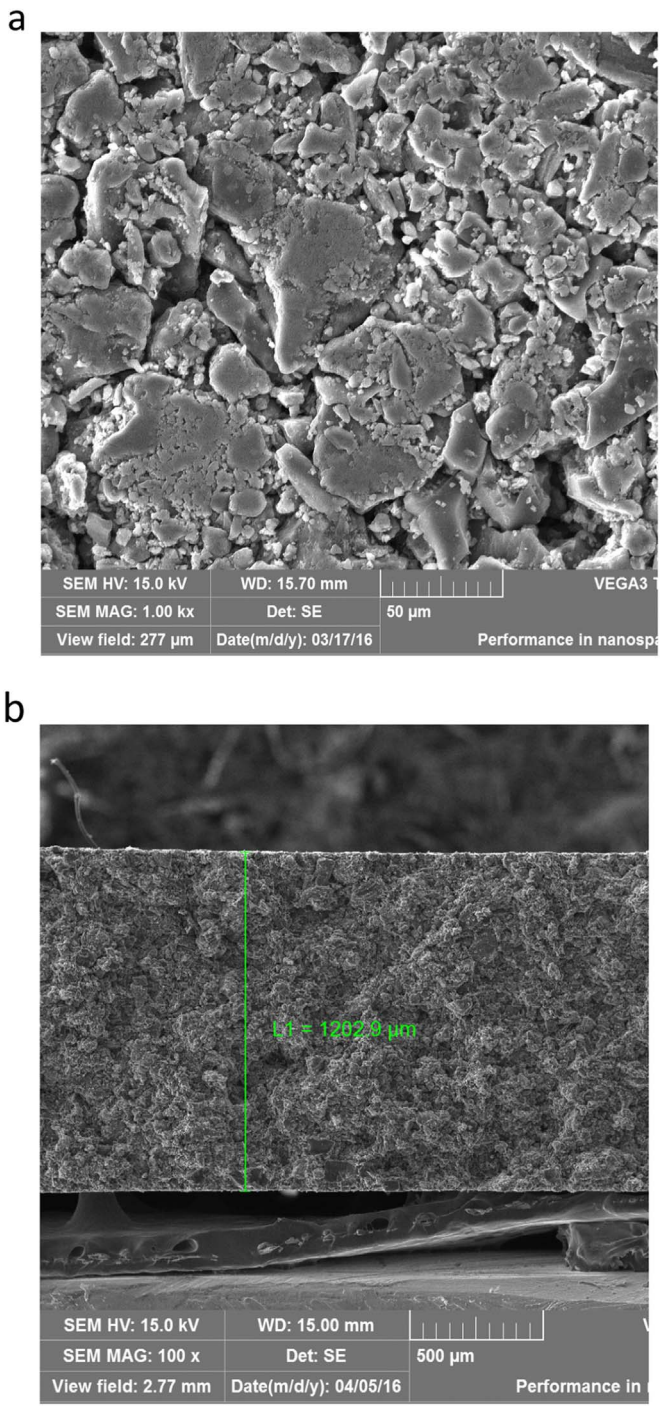

Fig. 9. (a) SEM image of AC/PVA disk on the surface. (b) SEM image of a section of the disk.

$2.76{\cdot}10^{16}$. The value of N_i is calculated by integrating over time the currents registered in FC1, before mass selection. When using the Surface Ion Source, the presence of other ionized atoms is negligible. The purity of the beam was anyway checked by means of mass scans, described as below.

The trend of the ionization tests can be seen in Fig. 10. At the beginning of the test (before t = 0), the ion source was heated up to its initial temperature (about 2200 °C); then, the oven was heated very slowly to obtain the strontium atoms evaporation. At every increase of oven temperature a sharp increase in beam current can be observed, until the maximum oven temperature, which corresponds to a current of about 80 A. From this point on a slow decrease is observed down to a few nanoamperes, indicating the complete evaporation of all the material contained in the MM.

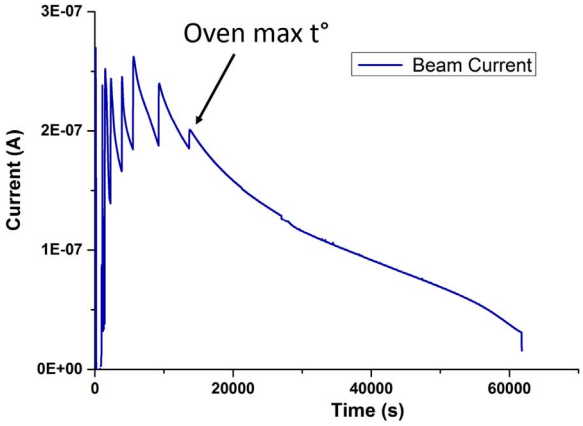

Fig. 10. Trend of strontium beams during tests. In the first part sharp peaks reflect oven heating steps. Once the maximum oven temperature is reached the beam current slowly decreases with the consumption of the deposited strontium.

During all the tests the strontium ion beam was optimized in terms of its focusing by means of the three quadruples (Q1–Q3) and deflectors (S1–S4) with the aim of focusing the beam on the emittance meter, which is the closest diagnostic device to the secondary target.

In Fig. 11 a mass scan is illustrated. From this data the percentage of strontium in the beam for the estimation of ε_s was calculated. Three relevant peaks have been considered: one of potassium (K_1) and the two main peaks of strontium (Sr_1 and Sr_2, attributed to masses 86–87 and 88, respectively). The total amount of strontium was 98.18%, so $\varepsilon_s = 0.9818$.

From the mass scan the magnetic field to be set by the Wien Filter in order to allow the selective passage of strontium ions was also determined.

In order to obtain a quantifiable amount of strontium in the NaCl substrate, the irradiation test was carried out taking into account the calculated ionization and separation efficiencies (ε_i = 0.1004 and $\varepsilon_s = 0.9818$) and applying Eq. (1) to extrapolate N_{MM}, that resulted in $9.46{\cdot}10^{17}$. The limit of quantification of the chosen analytical technique required a sample of at least $9.32{\cdot}10^{16}$ atoms of strontium, equivalent to 10 ppb (10 µg/L) after the target dissolution. For this reason, 140 µL of strontium standard solution (1 g/L) were introduced in the MM, volume containing the desired numbers of atoms of strontium.

During the test, the Faraday Cup was rapidly inserted into the beam line to detect the instantaneous strontium ion beam current, as a monitoring procedure. By the integration of the curve obtained with these experimental points, the number of Sr^{1+} ions impinging on the sodium chloride substrate was obtained. The deposition test lasted 15 h, at the end of which no strontium residual current could be detected (current below < 15 nA, considered the background threshold). The integration of the curve allowed the determination of the charge and thus the number of strontium atoms impinging on the NaCl substrate (N_t); the values are reported in Table 2.

At the end of the deposition, the substrate was removed from the channel and dissolved in HNO_3 0.3 M for quantitative analysis. The analysis allowed the determination of 10.09 µg/L of strontium by means of the calibration curve (y = mx + q, m = 0.0085, q = −0.004, r^2 = 0.995). The calibration curve is represented in Fig. 12, the red dot represents the sample value.

The strontium recovered from the substrate was calculated to be 4.0361 µg, corresponding to $4.606{\cdot}10^{-8}$ mol and $2.774{\cdot}10^{16}$ atoms. So the recovered strontium was 41.1% of the integrated charge, as reported in Table 2.

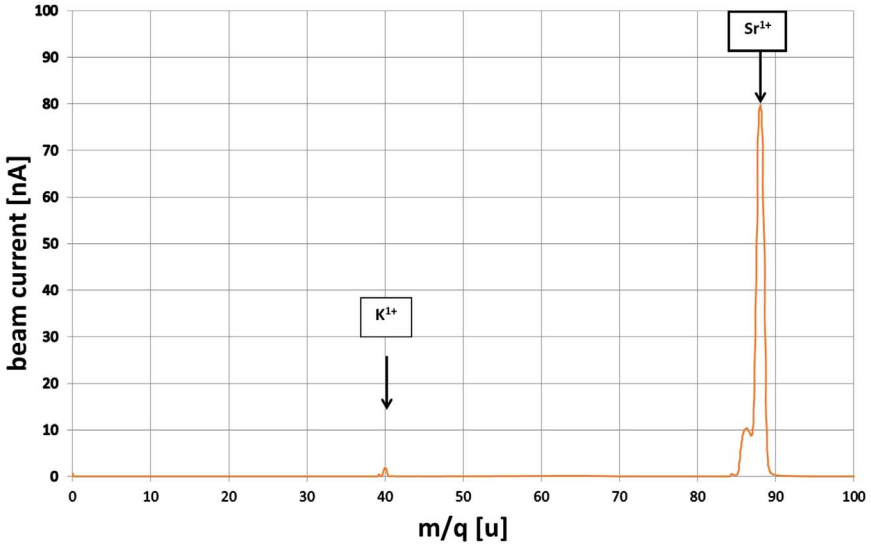

Fig. 11. This graph represents the mass profile of the beam when introducing a MM charged with strontium nitrate. Due to the good selectivity of SIS, almost only strontium isotopes peaks can be observed.

Table 2
Integrated charge is the value in Coulomb derived from the integration of beam current over time. From it the total number of atoms (N_t) is calculated. The deposited strontium and yttrium atoms are experimentally determined by GF-AAS and ICP-AES after target dissolution. Efficiency is then calculated as percentage.

Element	Integrated charge (C)	N_t	Deposited atoms	Atoms recovered from the substrate
Strontium	$1.1 \cdot 10^{-2}$	$6.8 \cdot 10^{16}$	$2.8 \cdot 10^{16}$	41.1%
Yttrium	$1.3 \cdot 10^{-4}$	$8.0 \cdot 10^{14}$	$8.0 \cdot 10^{14}$	100.0%

6.2.2. *Yttrium*

Yttrium beam production has been plagued by difficult atom evaporation. Yttrium has a very high boiling temperature. At atmospheric pressure its boiling point is 3370 °C; this value decreases when operating in vacuum conditions ($5 \cdot 10^{-6}$ mbar), reaching the value of 1600 °C (Honig, 1962). To overcome this limiting factor two different possibilities where studied: (i) the choice of the most volatile yttrium salt and (ii) the positioning of the MM in the hottest region of the ion source without folding it as in the case of strontium.

Preliminary tests with the conventional MM system were not successful; very low beam currents were produced. For this reason, tests were later performed positioning the MM in the transfer line (40 mm from the gas injection and very close to the hot cavity), after folding the MM only once.

As already mentioned, the Plasma Ion Source (PIS) was used to ionize yttrium. The crucial parameters for this kind of apparatus are described here. Firstly, the transfer line (later only line) temperature, which is responsible for yttrium evaporation; the heating of the line influences the cathode temperature as well. The electron current is influenced also by the anode potential, which is fixed at 150 V. Moreover, a constant argon flux is used for plasma formation. To increase the ionization efficiency a small axial magnetic field (current 5 A, max voltage 30 V) was produced in the anode region, with a coil surrounding the ion source. The magnetic field improves the ion source performances by means of a plasma confinement effect. The ion beam extraction was set at 25 kV. Since the oven was not used (MM placed directly in the transfer line), the only way to control yttrium evaporation was the transfer line heating, which also controlled the electron current, and so yttrium ionization. As can be observed from picture 13, sharp peaks are present in the trend of the yttrium beam current throughout the deposition test, corresponding to the imposed increases in the cathode temperature. The cathode was heated up by 420 A in order to obtain yttrium evaporation and ionization; at 380 A the temperature has been proved to be above 2000 °C (Manzolaro et al., 2016). The use of the same numerical method allowed the calculation of the temperature of the transfer line at 420 A which turned out to be higher than 2200 °C.

To verify that no interfering mass 89 atoms, i.e. the mass of stable yttrium, were present in the beam before yttrium introduction, several mass scans were performed at each line current, from 350 A to 420 A. From 350 A, electron current is detected and a consistent ion beam is

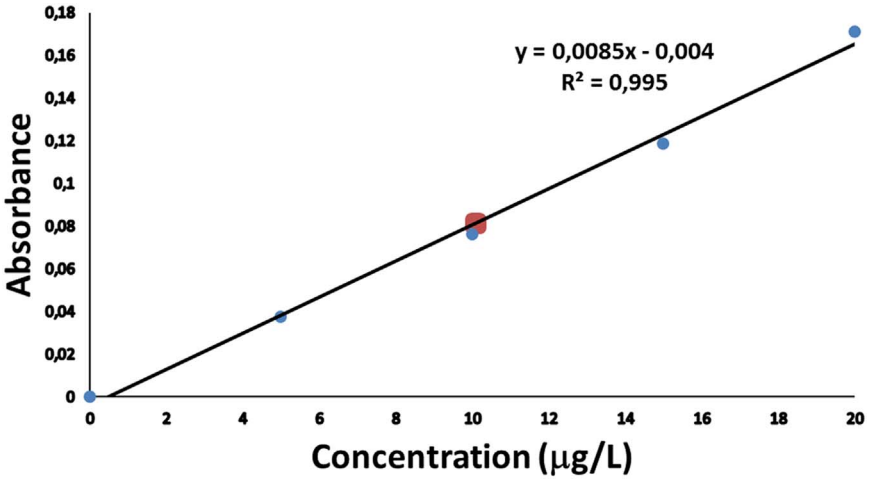

Fig. 12. Calibration curve used for strontium quantification. The curve was obtained with standards having the same matrix of the sample, the high amount of sodium chloride caused a little decrease in sensibility. The red spot corresponds to the analyzed sample. (For interpretation of the references to color in this figure legend, the reader is referred to the web version of this article.)

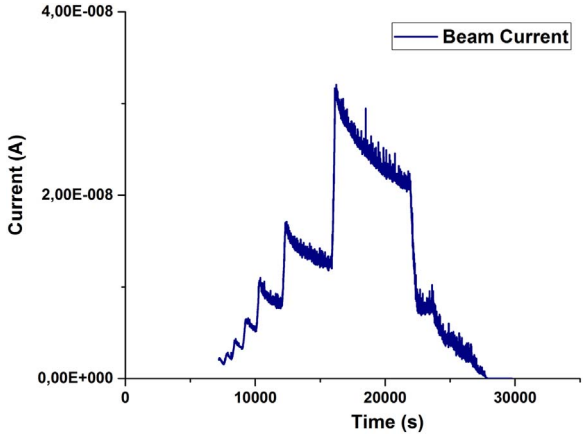

Fig. 13. Trend of yttrium beams during tests. It differs from strontium (Fig. 10) because: (i) no oven system was used, (ii) PIS was used. In this case each sharp peak corresponds to the increase in the cathode temperature.

produced. A representative mass scan is presented in Fig. 14a. As can be observed, no peak was detected corresponding to mass 89. Fig. 14b, instead, shows a mass scan obtained after the introduction of YCl_3 in the MM. Also in this case, the magnetic field for yttrium mass selection was extrapolated.

Tests were performed to compare yttrium nitrate and chloride as possible species to introduce in the mass marker. As can be observed from the graph of Fig. 15, yttrium chloride gives beam currents higher than those obtained with the nitrate at similar anode currents, i.e. cathode temperatures. For this reason YCl_3 was chosen for the deposition tests.

As in the case of strontium, before performing deposition some tests were performed to monitor the trend of the beam current with increasing cathode temperatures, as reported in Fig. 13. The integration of the curve made it possible to calculate the number of atoms in the beam, $N_t = 1.62 \cdot 10^{15}$.

Assuming that the sodium chloride disk is dissolved in a volume of 10 mL, a concentration of about 24 μg/L was expected in the solution. ICP-OES turned out to be a precise and accurate technique in this concentration range.

For the final deposition experiments, a MM was charged with 900 μL of YCl_3 water solution (1 g/L) and introduced into the transfer line. The Wien Filter was set to allow the passage of mass 89 only. As in the case of strontium, the Faraday Cup was inserted for a short time to intercept the beam periodically in order to quantify the yttrium current. The trend is extrapolated in Fig. 16; the curve was integrated obtaining the values reported in Table 2. After irradiation, the substrate was dissolved in 10 mL of HNO_3 0.1 M to verify yttrium deposition by means of ICP-OES. The results of the analysis are given in Table 2.

6.2.3. Iodine

Iodine beams were produced by the SPES FE for the first time. The ionization efficiency of iodine with the SPES PIS was not known so

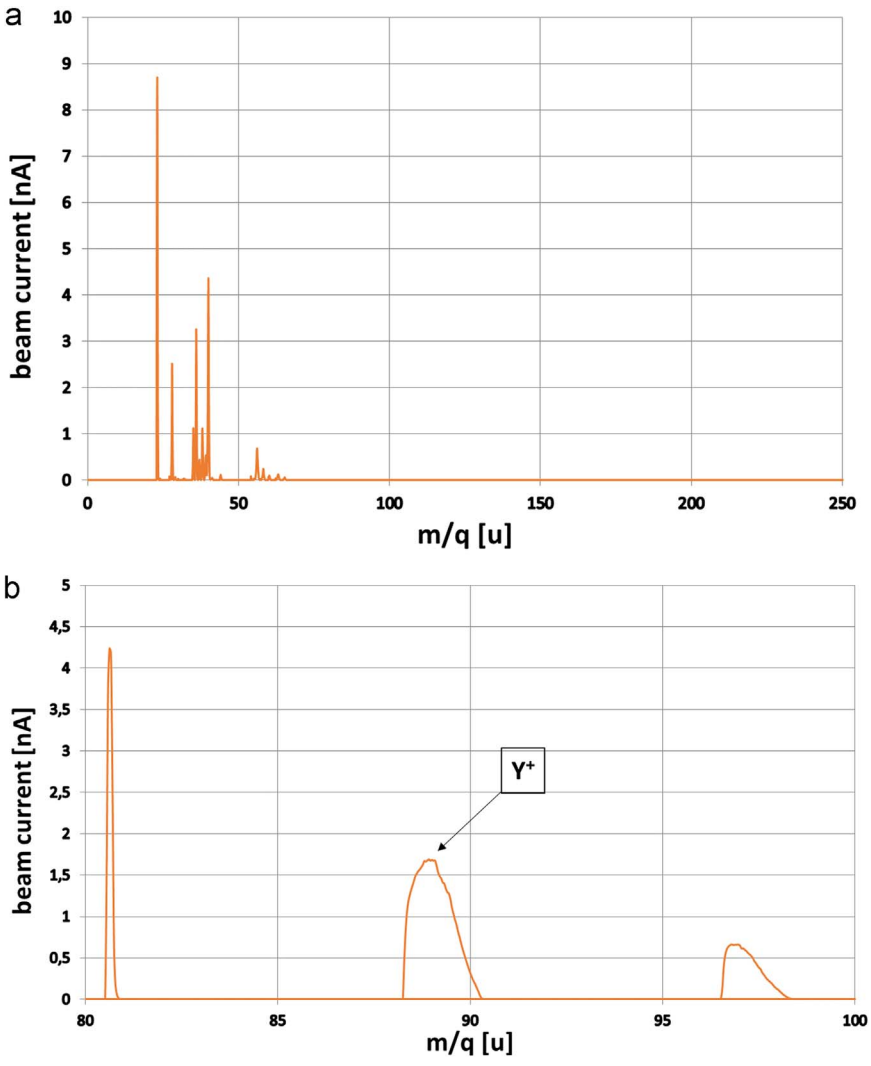

Fig. 14. Mass scans performed during yttrium ionization tests. In Fig. 14a a mass scan was performed before the introduction of yttrium into the FE to prove that no interfering masses were present close to yttrium mass. In Fig. 14b the zoom in the region of yttrium mass outlines the presence of yttrium in the beam, after yttrium introduction in the ion source.

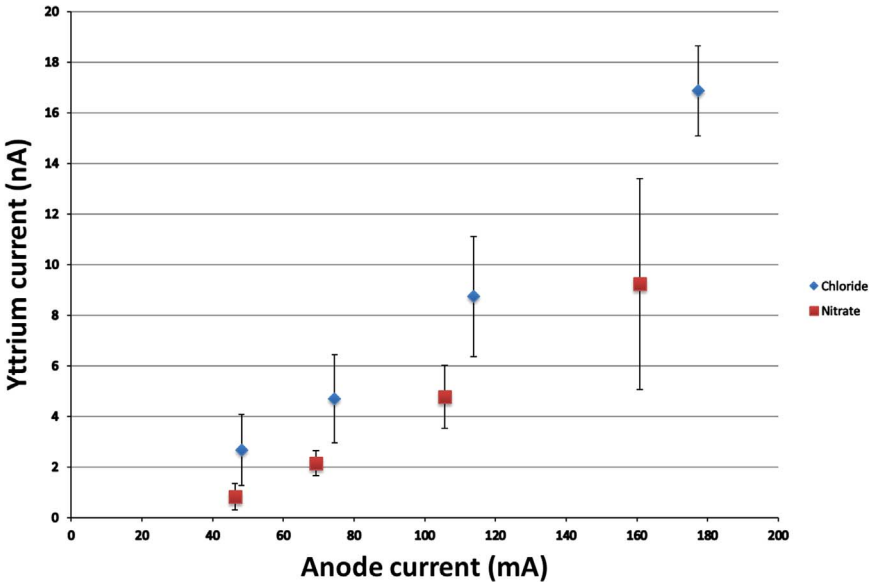

Fig. 15. In this graph a comparison between the yttrium currents in the chloride vs the nitrate form is made. To make a meaningful comparison, the yttrium currents were evaluated at similar anode currents. For each value the chloride gives always higher currents.

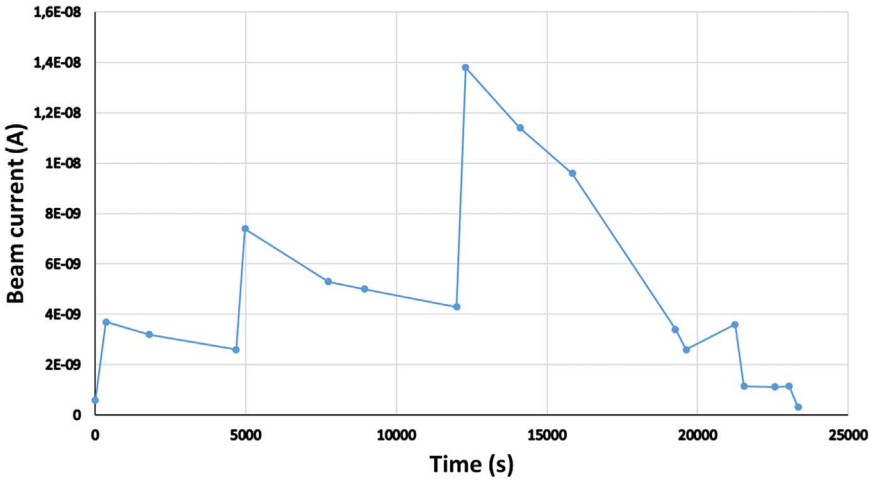

Fig. 16. Yttrium beam trend during a deposition test. The FC2 was inserted at certain times (blue dots) to monitor the beam. Integration of the curve gives the number of ionized atoms that reach the deposition substrate. (For interpretation of the references to color in this figure legend, the reader is referred to the web version of this article.)

three tests were performed to evaluate it. 40 µL of a solution of potassium iodide (1 g/L), freshly prepared by dissolving potassium iodide (Sigma Aldrich) in mQ water, were placed in the marker for the ionization tests. Efficiency turned out to be 19.34% (SD = 0.34) when operating with the cathode at 400 A. Iodine evaporation was efficiently controlled by means of the oven heating. No close interfering masses were observed as shown in Fig. 17. The iodine beam profile over time was very similar to that of strontium, with iodine ionization starting at oven currents of 10 A.

Analytical methods and the iodine recovery process from the AC/PVA matrix were set. More than 90% of iodine could be recovered following treatment with 0.5 M NaOH; the Limit of Quantification (LOQ) for iodine analysis was $3{\cdot}10^{-8}$ mol of I^-.

In contrast to the previous deposition test, the beam current was continuously monitor on the activated carbon substrate (here named FC3) during the test. Carbon is, indeed, a conductive material so the substrate was used as a homemade FC. The home made FC had no suppression electrode, so a correcting factor for the count of the exact iodine current had to be applied. The factor was calculated by monitoring the beam current on the suppressed FC and on the FC3, since they are very close and beam focalization parameters are the same. The AC/PVA substrate turned out to register 12,9% more current than the suppressed FC. This was kept under consideration for the following calculations.

Three deposition tests for iodine were carried out; the beam trend for the first test is outlined in Fig. 18 and data reported in Table 3. N_{MM} is the number of atoms deposited in the MM and was calculated by taking into account iodine ionization efficiency, the extraction process efficiency and the limit of quantification of the analysis. N_t is the number of iodine atoms reaching the AC/PVA target and is calculated from the integration of the FC3 signal over time, applying the aforementioned suppression correction. Following extraction, iodine was titrated and the final quantification and efficiency data are reported in Table 3.

7. Discussion

In order to produce stable beams of the atoms of interest the SPES test bench, named Front End, was used in off-line mode to perform tests by means of the Mass Marker technique. It was possible to produce strontium and iodine ion beams with good ionization efficiencies as previously demonstrated at the SPES laboratory: for strontium $\varepsilon_I > 10\%$ and for the first time for iodine $\varepsilon_i > 19\%$. It was also possible to ionize and detect yttrium ions, but the ionization efficiency for yttrium was very low, probably due to its poor volatility.

To collect the accelerated ions different substrates were designed and produced. The technical requirements to be fulfilled by the material were the mechanical resistance, the possibility to reach pressure of $10^{-5}-10^{-6}$ mbar and the lack of toxicity. The materials were also selected according to the requirement of making the transformation of

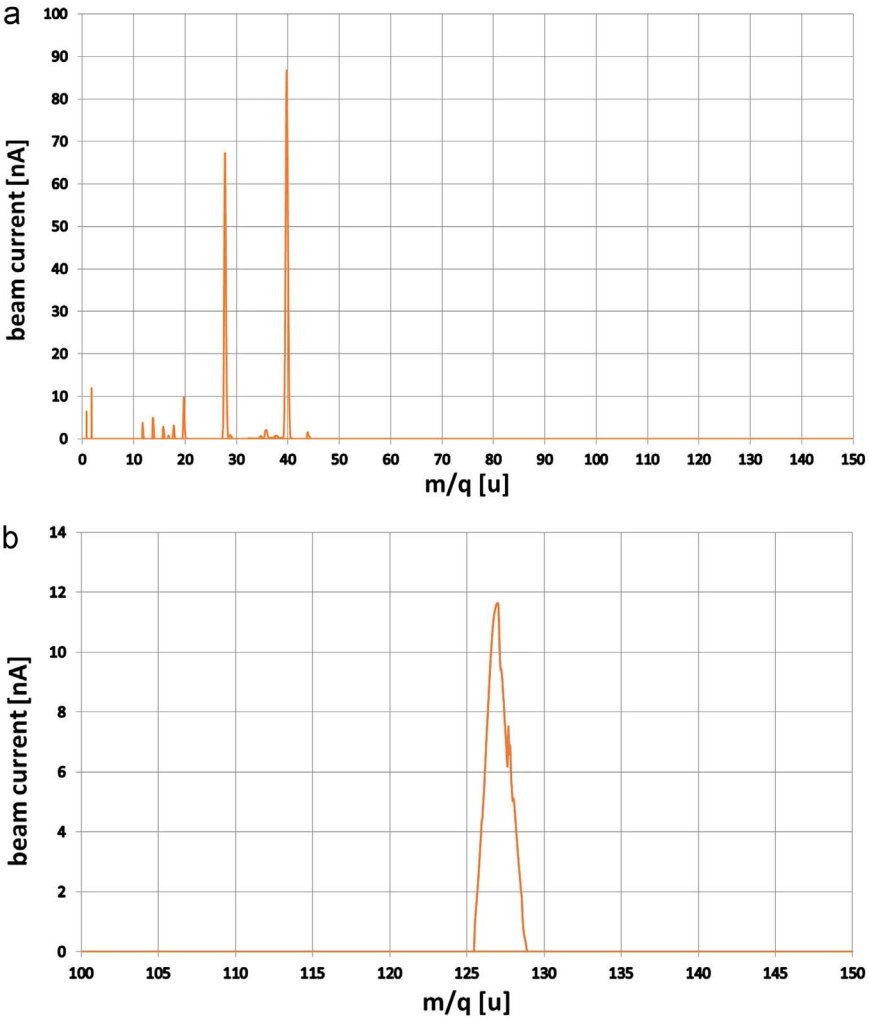

Fig. 17. As in the case of yttrium, mass scans were also performed for iodine during ionization tests. In Fig. 17a a mass scan was performed before the introduction of iodine into the FE to prove that no interfering masses were present close to mass 127. In Fig. 17b the zoom in the region of iodine mass outlines the presence of iodine in the beam, after iodine introduction in the ion source.

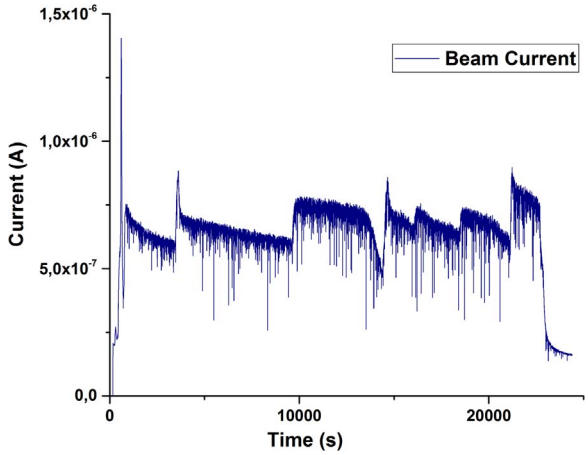

Fig. 18. Iodine currents during deposition test on the AC/PVA matrix. In this case the substrate was used as a FC so the quantity of iodine reaching the deposition substrate was monitored on line. Large fluctuations are due to the fact that the signal read on the substrate is unstable, because there is no electron suppression electrode.

the substrate into a radiopharmaceutical as easy and direct as possible. Moreover, the presence of isobaric contaminants was also considered as a criterion of choice to avoid the addition of stable contaminants derived from the collecting substrate material.

Among the biocompatible materials sodium chloride was chosen for the deposition of two of the tested elements: strontium and yttrium. In the case of the future production of ^{89}Sr, no isobaric impurities will be present in the beam and in the target material, simplifying the process. It will consequently be possible to dissolve the irradiated substrate in a proper water volume in order to obtain, in a single pass, a solution containing the dose of radiopharmaceutical. A crucial point remains the osmolarity of the solution after the dissolution of sodium chloride; for this reason, a process for the removal of the excess of sodium in solution might be considered essential. In the case of ^{90}Y production, instead, the presence of contaminants can not be avoided with mass separation, because of the long half-life of ^{90}Sr. For this reason the purification process of yttrium from strontium is currently under study at the Department of Pharmaceutical and Pharmacological Sciences of Padua University.

For iodine deposition activated carbon was chosen as the secondary

Table 3
Results of iodine depositions tests. N_t is the number of iodine ions impinging on the AC/PVA target and it is calculated from integration of the currents read directly from the deposition target. The number of extracted Iodine atoms is experimentally determined after extraction from the deposition target and titration. Efficiency is then calculated as the percentage of the iodine atoms extracted out of the total number of iodine atoms impinging the AC/PVA target (N_t). The number of atoms on the Mass Marker is different between test 1 and 2 and test number 3, because of a slightly different concentration of the starting KI solution, freshly prepared before the deposition.

	N_{MM}	N_t	Iodine atoms extracted from the target	Chemical recovery from the target
1st test	$5.5{\cdot}10^{17}$	$9.4{\cdot}10^{16}$	$2.1{\cdot}10^{16}$	22.7%
2nd test	$5.5{\cdot}10^{17}$	$9.9{\cdot}10^{16}$	$1.7{\cdot}10^{16}$	17.2%
3rd test	$7.5{\cdot}10^{17}$	$1.9{\cdot}10^{17}$	$1.2{\cdot}10^{17}$	63.7%

target material. Sodium chloride could not be used because it has, as an intrinsic contaminant, iodine in the anion forms of iodate and iodide. In the future this could represent a huge problem, since iodine contaminants would reduce specific activity. Different matrixes were taken into consideration in order to obtain an inert and iodine free compact substrate. Another problem to be taken into consideration is iodine volatility. Iodine in the molecular form is in the gaseous state at the operating pressure conditions ($10^{-5}-10^{-6}$ mbar) (Honig, 1962), thus possibly causing iodine ions to be lost immediately after being implanted in the secondary target. For this reason, activated carbon was chosen as an ideal material for matrix development, because it can effectively trap iodine molecules (Haefner and Tranter, 2007; Wilhelm and Deuber, 1991; Paviet-Hartmann et al., 2010). This material also allowed the use of the deposition target as a third Faraday Cup to continuously monitor the beam during the deposition tests.

The tests allowed depositing and recovering the implanted ions in all three cases. The recovery process proved to be simple and the use of compatible materials as secondary targets makes the presence of impurities negligible. The possibility to start from very pure materials for the production of these targets overcomes the problem of metallic impurities, which usually come from conventional metallic targets and present a problem in the radiolabeling process of targeting molecules for diagnosis and therapy. The only possible contaminants come from the irradiation process because of the presence of isobaric and pseudo isobaric nuclides that have to be eliminated through an adequate chemical process.

The calculated values of efficiency for the deposition of the beam on the designed substrates were above 40% for strontium and yttrium, thus indicating quite a good recovery of the ions accelerated in the beam. In the case of strontium efficiency was of 41%. The deposition test was however carried out without the possibility of monitoring Sr^{+} currents during the test, because the FC was left outside the beam line so as not to intercept the ion beam. Consequently the predicted number of ions reaching the target is only indicative because it does not consider possible fluctuations in the beam current. Moreover, in the case of strontium, another important factor must be taken into consideration: stable strontium is an isotopic mixture (^{84}Sr 0.56%, ^{86}Sr 9.86%, ^{87}Sr 7.0% and ^{88}Sr 82.58%) so, by selecting mass 88, the other strontium isotopes were after mass selection. On the target, after irradiation, the spot of the beam had a horizontal elongated shape, that was not completely centered on the NaCl disk.

In the case of yttrium the recovery was extremely efficient, since all the foreseen yttrium ions reaching the target could be later detected by ICP-OES.

In the case of iodine the efficiency of recovery was greatly increased in the last deposition test. This was due to the different treatment of the irradiated substrate that was treated with sodium hydroxide for a longer time (120 min instead of 15) and above all at a higher temperature (55 °C instead of room temperature). Higher temperatures and longer time might be useful to reach a recovery of 100%.

8. Conclusions

This study proves that the beams produced with the ISOL method can be easily used for the obtainment of pure nuclides. Stable ion beams of the desired elements were efficiently produced and ions recovered thanks to the deposition on suitable targets. The chemical purification process for the elimination of isobaric contaminants is now under study. The ISOL method opens the possibility to produce a wide range of radionuclides with extremely high levels of purity both in terms of specific activity, because of the lack of isotopic contaminants, and radionuclidic and chemical purity, since impurities coming from the beam and from the targets are very limited, compared to those of traditional methods.

Acknowledgements

Authors would like to thank G. D'Odorico and C. Todesco of the University of Padova for their precious scientific and technological support in yttrium and iodine beams study and professor V. Di Noto and K. Vezzù for their precious help in yttrium ICP analysis.

References

Al-Busafi, S., Ghali, P., Wong, P., Novales-Diaz, J.A., Deschênes, M., 2012. The utility of Xenon-133 liver scan in the diagnosis and management of nonalcoholic fatty liver disease. Can. J. Gastroenterol. 26, 155–159.
Al-Khalili, J., Roeckl, E., 2006. The Euroschool Lectures on Physics with Exotic Beams 2 Springer, Berlin.
Azaiez, F., Bracco, A., Dobeš, J., Jokinen, A., Körner, G.E., Maj, A., Murphy, A., Van Duppen, P. (Eds.), 2014. Nuclear Physics for Medicine. NuPECC (ISBN: 9782368730089).
Chamarthy, M.R., Williams, S.C., Moadel, R.M., 2011. Radioimmunotherapy of Non-Hodgkin's Lymphoma: from the 'Magic Bullets' to 'Radioactive Magic Bullets'. Yale J. Biol. Med. 84, 391–407.
Corradetti, S., Biasetto, L., Manzolaro, M., Scarpa, D., Carturan, S., Andrighetto, A., Prete, G., Vasquez, J., Zanonato, P., Colombo, P., Jost, C.U., Stracener, D.W., 2013. Neutron-rich isotope production using a uranium carbide – carbon nanotubes SPES target prototype. Eur. Phys. J. A 49, 56.
Crepieux, B., Kirkby, L., 2006. Préparation et domaine des mass-marker des cibles ISOLDE, Internal report, CERN.
Di Noto, V., Ni, D., Dalla Via, L., Scomazzon, F., Vidali, M., 1995. Determination of platinum in human blood using inductively coupled plasma atomic emission spectrometry with an ultrasonic nebulizer. Analyst 120, 1669–1673.
Frech, W., Cedergreen, A., 1977. Investigation of reactions involved in flameless atomic absorption procedures part III. A study of factors influencing the determination of lead in strong sodium chloride solutions. Anal. Chim. Acta 88, 57–67.
Goffredo, V., Paradiso, A., Ranieri, G., Gadaleta, C.D., 2011. Yttrium-90 (90Y) in the principal radionuclide therapies: an efficacy correlation between peptide receptor radionuclide therapy, radioimmunotherapy and transarterial radioembolization therapy. Ten years of experience (1999–2009). Crit. Rev. Oncol. Hematol. 80, 393–410.
Haefner, D.R., Tranter, T.J., 2007. Methods of Gas Phase Capture of Iodine from Fuel Reprocessing Off-Gas: A Literature Survey, Idaho National Laboratory - INL/EXT-07-12299.
Handbook of Nuclear Chemistry, 2011. Springer, doi: 10.1007/978-1-4419-0720-2.
Honig, R.E., 1962. Vapor pressure data for the solid and liquid elements. RCA Rev. 23, 567–586 Radio Corporation of America.
Kaghazchi, T., Kolur, N.A., Sabet, R.H., 2009. Recovery of iodine with activated carbon from dilute aqueous solutions. Afinidad 542, 338–343.
Kuroda, I., 2012. Effective use of strontium-89 in osseous metastases. Ann. Nucl. Med. 26, 197–206.
Lozano-Castelló, D., Cazorla-Amorós, D., Linares-Solano, A., Quinn, D.F., 2002. Activated carbon monoliths for methane storage: influence of binder. Carbon 40, 2817–2825.
Manzolaro, M., Meneghetti, G., Andrighetto, A., Vivian, G., D'Agostini, F., 2016. Thermal-electric coupled-field finite element modeling and experimental testing of high-temperature ion sources for the production of radioactive ion beams. Rev. Sci. Instrum. 87, 02B502. http://dx.doi.org/10.1063/1.4933081.
Manzolaro, M., Andrighetto, A., Meneghetti, G., Rossignoli, M., Corradetti, S., Biasetto, L., Scarpa, D., Monetti, A., Carturan, S., Maggioni, G., 2013. Ionization efficiency estimations for the SPES surface ion source. Nucl. Instrum. Methods Phys. Res. 317, 446–449. http://dx.doi.org/10.1016/j.nimb.2013.07.045.
Manzolaro, M., Andrighetto, A., Meneghetti, G., Monetti, A., Scarpa, D., Rossignoli, M., Vasquez, J., Corradetti, S., Calderolla, M., Prete, G., 2014. Ongoing characterization of the forced electron beam induced arc discharge ion source for the selective production of exotic species facility. Rev. Sci. Instrum. 85, 02B918. http://dx.doi.org/10.1063/1.4857175.
Manzolaro, M., Meneghetti, G., Andrighetto, A., 2010. Thermal-electric numerical simulation of a surface ion source for the production of radioactive ion beams. Nucl. Instrum. Methods Phys. Res. 623, 1061–1069.
Mathews, J.J., Maurer, A.H., Steiner, R.M., Marchetti, N., Criner, G., Gaughan, J.P., Coxson, H.O., 2008. New 133Xe gas trapping index for quantifying severe emphysema before partial lung volume reduction. J. Nucl. Med. 49, 771–775.
Monetti, A., Andrighetto, A., Petrovich, C., Manzolaro, M., Corradetti, S., Scarpa, D., Rossetto, F., Martinez Dominguez, F., Vasquez, J., Rossignoli, M., Calderolla, M., Silingardi, R., Mozzi, A., Borgna, F., Vivian, G., Boratto, E., Ballan, M., Prete, G., Meneghetti, G., 2015. The RIB production target for the SPES project. Eur. Phys. J. A 51, 128.
Moulay, S., 2013. Molecular iodine/polymer complexes. J. Polym. Eng. 33, 389–443.
Nilsson, T., 2013. European RIB facilities – status and future. Nucl. Instrum. Methods B 317, 194.
Paviet-Hartmann, P., Kerlin, W., Bakhtiar, S., 2010. Treatment of gaseous effluents issued from recycling: A review of the current practises and prospective improvements, Idaho National Laboratory - INL/CON-10-19961.
Prell, L.J., Styris, D.L., 1991. Mechanism of electrothermal atomization for yttrium by mass spectrometry. Spectrochim. Acta 46, 45–49.
Rodrigues, G., Yao, X., Loblaw, D.A., Brundage, M., Chin, J.L., 2013. Low-dose rate brachytherapy for patients with low- or intermediate-risk prostate cancer: a

systematic review. Can. Urol. Assoc. J. 7, 463–470.
Rowe, R.C., Sheskey, P.J., Cook, W.G., Fenton, M.E., 2012. Handbook of Pharmaceutical Excipients, 7th edition.
Schwarz, S.B., Thon, N., Nikolajek, K., Niyazi, M., Tonn, J., Belka, C., Kreth, F., 2012. Stereotactic Brachytherapy for Brain Tumors, in "Brachytherapy". Kazushi Kishi, InTech.
Shi, F., Zhang, X., Wu, K., Gao, F., Ding, Y., Maharjan, R., Zhang, R., Zhang, F., Li, C., 2014. Metastatic malignant melanoma: computed tomography-guided 125I seed implantation treatment. Melanoma Res. 24, 137–143.
Schwellnus, F., Catherall, R., Crepieux, B., Fedosseey, V.N., Marsh, B.A., Mattolat, Ch, Menna, M., Oesterdahl, F.K., Raeder, S., Stora, T., Wendt, K., 2009. Study of low work function materials for hot cavity resonance ionization laser ion sources. Nucl. Instrum. Methods Phys. Res. B 267 (10), 1856–1861.
Welch, M.J., Redvanly, C.S., 2003. Handbook of Radiopharmaceuticals, Radiochemistry and Applications. Wiley & Sons Ltd, Chichester(Eng).
Wien, W., 1897. Verhandlungen Physik 16. Gesellsch, Berlin, pp. 165.
Wien, W., 1902, Ann. Physik 8, 260.
Wilhelm, J.G., Deuber, H., 1991. The removal of short-lived iodine isotopes. In: Goossens, W.R.A., Eichholz, Geoffrey G. (Eds.), Treatment of Gaseous Effluents at Nuclear Facilities. Harwood Academic Publishers.
Wolf, B., 1995. Handbook of Ion Sources, GSI Center for Heavy Ion Research. Darmstadt, Germany.
Wyszomirska, A., 2012. Iodine-131 for therapy of thyroid diseases. Physical and biological basis. Nucl. Med. Rev. 15 (2), 120–123.